Original Article

ZR-75-1 breast cancer models to study the utility of ^{18}F-FES by PET imaging

Ziteng Ding[#], Xudang Xu[#], Tiannv Li, Jia Wang, Jin Sun, Lijun Tang

Department of Nuclear Medicine, The First Affiliated Hospital with Nanjing Medical University, Nanjing, China

Contributions: (I) Conception and design: Z Ding, X Xu, J Sun; (II) Administrative support: L Tang; (III) Provision of study materials or patients: T Li, J Sun, J Wang; (IV) Collection and assembly of data: Z Ding, X Xu; (V) Data analysis and interpretation: Z Ding, X Xu, J Sun; (VI) Manuscript writing: All authors; (VII) Final approval of manuscript: All authors.

[#]These authors contributed equally to this work.

Correspondence to: Lijun Tang; Jin Sun. Department of Nuclear Medicine, The First Affiliated Hospital with Nanjing Medical University, Nanjing, China. Email: tanglijun@njmu.edu.cn; wander21@126.com.

Background: Breast cancer is a hormone-dependent tumor, and 70–80% of breast cancer patients are estrogen receptor (ER) positive. ZR-75-1 cell lines are more consistent with human breast cancer, which is mostly ER positive and PR positive. To better study the biological characteristics of ^{18}F-fluoroestradiol (^{18}F-FES) in breast cancer patients, ZR-75-1 breast cancer models were selected to provide a basis for further clinical application.

Methods: ^{18}F-FES uptake *in vivo* was evaluated in ZR-75-1 tumor-bearing mice, using MCF-7 tumor-bearing mice as a positive control. Competitive inhibition experiment was also performed, using ER down-regulator fulvestrant. Biodistribution of ^{18}F-FES was observed in ZR-75-1 breast tumor-bearing mice scanning by ^{18}F-FES-PET/CT *in vivo* and γ counter *ex vivo*. The expression of ER was also determined by immunohistochemistry. An abnormal toxicity test was performed in ICR male mice whose behavior and vital signs were observed within 48 hours of ^{18}F-FES injection. OLINDA/EXM 2.0 software was used to calculate the absorbed doses of adult female body phantoms.

Results: There was no significant difference in FES uptake between ZR-75-1 and MCF-7 tumor-bearing mice. Intervention with fulvestrant decreased the uptake of ^{18}F-FES. Biodistribution studies demonstrated that the uptake of ^{18}F-FES was high in the liver and kidneys but low in the brain. Other than excretory organs, the uptake of ^{18}F-FES in ER-positive breast tumors was significantly higher than in ER-negative tissues. The estimated human effective dose was 0.016 mSv/MBq for the adult female body model.

Conclusions: The ^{18}F-FES tracer could have suitable properties for imaging ER-positive breast tumors. It may provide an important evidence for individualized treatment of patients with breast cancer.

Keywords: Breast cancer; ^{18}F-FES-PET/CT; biodistribution; immunohistochemistry; safety

Submitted Nov 08, 2020. Accepted for publication Jan 15, 2021.
doi: 10.21037/tcr-20-3228
View this article at: http://dx.doi.org/10.21037/tcr-20-3228

Introduction

Breast cancer is one of the most common causes of cancer-related death in the world. There were an estimated 2.1 million new cases of breast cancer worldwide in 2018, accounting for 11.6% of all new cancer patients (1). Besides, it alone accounts for 30% of female new cancer cases in the United States of 2020 (2). Increasing evidence shows that breast cancer is a hormone-dependent tumor. Estrogen receptor (ER), located in cell nuclei of target tissues, is positive in 70–80% of breast cancers (3). It plays a key role in cell proliferation, survival and invasion and is one of therapeutic targets for breast cancer (4). Therefore, monitoring ER levels is necessary to predict the efficacy of

therapy and prognosis for breast cancer (5).

At present, ER expression is detected by immunohistochemistry (IHC), an invasive and semi-quantitative detection method (6). It is limited by the location of lesions and the risk associated with biopsy. There is significant heterogeneity due to different measurement methods within and between laboratories (7). In addition, 18–40% of patients with metastatic breast cancer have different expression of ER in primary and metastatic lesions (8). ER expression levels vary with the progress of the disease or endocrine therapy intervention. The American Society of Clinical Oncology and the American Society of Pathologists reported that 20% of global IHC measurements are inaccurate (9). In summary, IHC does not dynamically and comprehensively reflect the estrogen levels in patients (10).

Positron emission tomography (PET) is a non-invasive whole-body imaging application. ^{18}F-fluoroestradiol (^{18}F-FES), an estrogen-based radiopharmaceutical, is the most widely studied ER-specific imaging agent. ^{18}F-FES-PET/CT can be used for noninvasive evaluation of the ER status in primary and metastatic lesions, thereby predicting the effect of endocrine therapy at an early stage and contributing to individualized therapy. ^{18}F-FES-PET/CT detects ER-positive tumor lesions with a high sensitivity (84%) and specificity (98%) (11).

MCF-7 cells, ER positive and progesterone receptor (PR) negative, were more widely used than ZR-75-1 in the study of ^{18}F-FES (12). While receptors of ZR-75-1 cells, ER positive and PR positive, were consistent with that of most breast cancer patients (13). To better study the biological characteristics of ^{18}F-FES in breast cancer patients, ZR-75-1 cells were selected in our study. We present the following article in accordance with the ARRIVE reporting checklist (available at http://dx.doi.org/10.21037/tcr-20-3228).

Methods

All animal experiments were approved by the Institutional Animal Care and Use Committee of MITRO Biotech (AP-MIJ190019), in compliance with all national or institutional guidelines for the care and use of animals.

Cell lines and culture

ZR-75-1 and MCF-7 cells were human breast cancer lines obtained from SuzhouShinno Biotechnology LDT. ZR-75-1 cells were cultured in RPMI 1640 medium and MCF-7 cells in DMEM medium, both contained 10% fetal bovine serum (Hyclone, USA).

Animals

ZR-75-1 and MCF-7 cells were inoculated subcutaneously (1×10^7cells) into the right mammary fat pad of female NOD/SCID mice (22 mice, 5–6 weeks, 17–22 g, Vital River, China). All mice were exposed to a 12-h light-dark cycle with the temperature and humidity were 20.71–24.70 ℃ and 47.8–67.7%. Estrogen pellets (0.36 mg, 60-day release, Innovative Research, USA) were implanted into the left shoulder one day before tumor cell inoculation and removed 3 days before scanning. The length and width of the tumor were measured every 3 days after inoculation. When tumors grew to 5mm in diameter, mice were included in the experiment. MCF-7 breast tumor-bearing mice (n=6) were served as positive control group of ^{18}F-FES uptake. ZR-75-1 breast cancer-bearing mice (n=6) were used to observe the biodistribution, immunohistochemistry and safety of ^{18}F-FES. The remaining mice were randomly divided into 2 groups (5/each group) for the competitive inhibition experiment.

Micro-PET/CT imaging

The radiosynthesis of ^{18}F-FES was synthesized in Department of Nuclear Medicine, The First Affiliated Hospital with Nanjing Medical University. Positron drug synthesis module TRACERlab FXFN synthesis of hardw (GE medical system, America) were imported the synthesis program. 3-O-(methoxy-methyl)-16,17-O-sulfonyl-16-epiesteriol (ABX, France) was used as the precursor. The radiochemical purity of ^{18}F-FES exceeded 98%, and the radiochemical yield synthesis was 36%±5% after decay correction.

Small-animal PET was performed on a micro-PET/CT (snpc-103, PENGSENG Healthcare, China). Mice were anesthetized with isoflurane (RWD Life Science, China), and 200 μCi of ^{18}F-FES dissolved in saline was injected in the tail vein. PET/CT scanning was performed 1 hour after injection. To observe the dynamic distribution of FES *in vivo* PET/CT scanning was performed at 15, 30, 60 and 120 minutes after FES injection. Mice inhaled isoflurane continuously to maintain the anesthesia effect. Three bed positions were acquired for 10–30 minutes each. The scanning energy window was 350–650 keV, tube voltage was 30–90 kVp and exposure time ≤10 s.

The images were reconstructed using PMOD software. For data analysis, the volume of interest (VOI) was manually drawn to cover various organs and the tumor on fused images. The range of VOI should be smaller than the actual size of organs to prevent the volume effect of adjacent organs. The percent injected dose per gram of tissue (%ID/g) and the target-to-muscle ratio (T/M) were calculated.

^{18}F-FES uptake in ZR-75-1 breast tumor-bearing mice

In vivo imaging of ZR-75-1 breast cancer bearing mice

Receptor-targeting images of ZR-75-1 tumor-bearing mice were acquired after injection of FES. We used MCF-7 tumor-bearing mice as a positive control and the scan was performed in the same way.

Competitive inhibition

A baseline ^{18}F-FES-PET/CT scan was performed 1 day before treatment (Day 0). Fulvestrant (Vetter Pharma-Fertigung GmbH & Co. KG, Germany) and saline (HeibeiTiancheng Pharmaceutical CO., LTD, China) were administered separately to the experimental and control groups. The program and dose for each group were as follows: intramuscular injection, fulvestrant 5 mg/mouse/week and saline 5 mL/kg/week (Day 1 and Day 8). ^{18}F-FES-PET/CT scan was performed 3 days after administration (Day 4 and Day 11).

Biodistribution of ^{18}F-FES

ZR-75-1 breast tumor-bearing mice were used for this study. PET/CT was performed at different time points as mentioned above.

The mice were euthanized immediately after ^{18}F-FES-PET/CT scanning. Tissue samples were removed and weighed, including tumor, heart, liver, spleen, lung, kidney, brain, uterus, ovary, muscle and femur. The radioactivity of the samples was determined in a γ counter (ATOMLAB^{TM} 500, BIODEX, USA).

Immunohistochemistry

^{18}F-FES-imaged tumor were fixed in 10% neutral-buffered formalin for 24 hours and sectioned in 4 to 5-mm-thick slices. All slices were incubated overnight with the monoclonal rabbit anti-ERα antibody (Abcam, Britain). On the second day, the slices were incubated with secondary biotinylated antibodies (Abcam, Britain). Dying with 3, 3' diaminobenzidine solution followed by counter staining with hematoxylin. Positive cells were brown. The results were qualitatively evaluated by two independent pathologists using the Allred scoring system (14). A score of 3–8 was considered positive.

Safety

Abnormal toxicity test

According to the abnormal toxicity test standard, ICR male mice (n=5) were injected with 0.5 mL of ^{18}F-FES via the tail vein and observed for 48 hours.

Radiation dose estimation in the human body

PET data were reconstructed. VOI was projected into the dynamic PET image, and time-activity curves of each organ were generated. After obtaining the curves, the radioactive retention time of each source organ in mice was calculated using PMOD by the formula:

$$\tau = \frac{\int_0^\infty A(t)\,dt}{A_0} \quad [1]$$

where A_0 is the applied activity and A (t) is the activity measured in organs. The remainder organ retention time was obtained from the maximum allowed by physics, which is 2.62 MBq.h/MBq for ^{18}F, minus the retention time of all source organs (15). According to the relative proportion of source organ mass and body weight in mice and the adult female body model, the radioactive retention time of each source organ of a 60-kg adult female model was calculated as follows (16):

$$(R_{Organ})_{huaman} = \frac{1}{n}\left\{\sum_{i=1,2,\ldots n}\left\{(R_{Organ})_{mice(i)} \times \left(\frac{M_{TB\ weight}}{m_{Organ}}\right) Mice(i)\right\}\right\} \times \left(\frac{m_{Organ}}{M_{TB\ weight}}\right) Human \quad [2]$$

where $(R_{Organ})_{huaman}$ is the human organ retention time, $(R_{Organ})_{mice(i)}$ is the corresponding organ retention time of the i-th mouse, $M_{TB\ weight}$ is body weight, and m_{Organ} is organ quality. The radioactive retention time of each source organ of the adult female body model was input in OLINDA/EXM 2.0 software to calculate the absorbed dose and effective dose of ^{18}F-FES in the human body.

Statistical analysis

Data were expressed as mean ± standard deviation. Independent sample t test was used to analyze FES uptake in tumor tissues at different stages and the competitive test. The Pearson correlation coefficient was calculated to determine the correlation between *in vivo* and *ex vivo* measurements. The radiation dose measured by us was compared with literature using paired *t*-test. Statistical calculation was performed using the SPSS 26.0 software. P<0.05 was considered statistically significant.

Results

The experimental scheme was successfully completed in n=22 animals. Tumor size in tumor-bearing mice increased gradually after inoculation with the cancer strain.

^{18}F-FES uptake in ZR-75-1 breast tumor-bearing mice

In vivo imaging of ZR-75-1 breast cancer bearing mice

FES uptake in MCF-7 and ZR-75-1 breast tumor-bearing mice are shown in *Figure 1*. There was no significant difference in FES uptake between the tumor-bearing mice (t=0.855, P=0.409). The %ID/g value of ZR-75-1 and MCF-7 breast tumor-bearing mice were 1.87±0.20 and 2.20±0.16 (t=0.33, P=0.75).

Competitive inhibition experiment

Based on baseline ^{18}F-FES-PET/CT scan results, there was no statistical difference in ^{18}F-FES uptake of tumors in the experimental and control groups (t=1.428, P=0.10). The %ID/g value of tumors in control groups were 1.47±0.34, 1.307±0.31 and 1.35±0.41 on 0, 4 and 11 days which were no statistically different (0 *vs.* 4 days, t=1.13, P=0.32; 4 *vs.* 11 days, t=0.98, P=0.38). After administration of fulvestrant, the %ID/g value of tumors were significantly lower than those at baseline (*Figure 2*). The %ID/g value of tumor were 0.79±0.16 and 1.77±0.33, respectively t=6.44, P=0.03). Moreover, after the second administration of fulvestrant, ^{18}F-FES uptake was significantly lower than those in saline group (t=2.84, P=0.047). These results indicated that fulvestrant has a significant competitive inhibition effect on the uptake of ^{18}F-FES in ER-positive tumors.

Biodistribution of ^{18F}-FES

The uptake and kinetics of ^{18}F-FES in ZR-75-1 breast tumor-bearing mice are shown in *Figure 3*. A great deal of ^{18}F-FES was taken up by the liver, gallbladder, intestine, kidneys and bladder, especially at 15 minutes after injection. ^{18}F-FES uptake in these primary metabolic and excretory organs peaked at 120 minutes after administration. The %ID/g values were 5.34±2.47, 41.09±26.40, 56.32±19.25, 3.76±2.98 and 65.46±33.94 respectively. ^{18}F-FES uptake in blood-rich organs including the heart and spleen peaked at 15 minutes after administration. ^{18}F-FES uptake also reached a maximum at 15 minutes after injection in other ER-negative tissues like the muscle and brain, and gradually decreased at later times. The uterus and ovary were too small to show *in vivo*.

At 15, 30, 60 and 120 minutes after administration, the %ID/g value of ER-positive tumors were 2.18±0.19, 2.31±0.19, 2.20±0.59 and 1.99±0.19, respectively. There were no statistical difference among ^{18}F-FES uptake in tumors at different times (F=0.70, P=0.56). ^{18}F-FES uptake in tumors was always higher than that in muscle. The T/M ratio increased gradually and reached the highest level (6.35±2.58) at 120 minutes after administration.

Time-radioactivity curves were made according to ^{18}F-FES uptake within 120 minutes in different organs and tissues, and the area under the curves (AUCs) were calculated: bladder > intestine > gallbladder > liver > kidney > tumor > spleen > heart > bone joint > lung > muscle > tibias > brain tissue.

There was a significant difference between the results of PET/CT scan *in vivo* and γ counter *ex vivo* in ZR-75-1 tumor-bearing mice (t=2.89, P=0.02). *In vivo*, the %ID/g value of tumors and muscle were 1.87±0.20 and 0.44±0.09. *Ex vivo*, the %ID/g value of tumors and muscle were 0.74±0.21and 0.23±0.03, respectively. Though later values were lower than former, the values were positively correlated (r^2=0.88). The %ID/g value of the uterus and ovaries *ex vivo* were 3.96±1.39 and 2.56±0.46, which were second only to that of the liver (the uterus and ovaries are

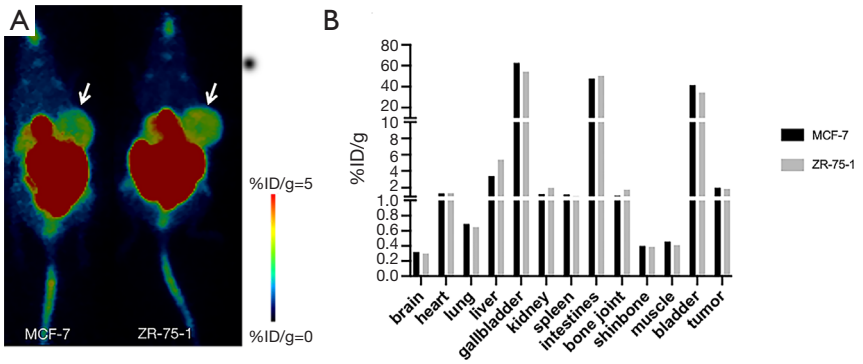

Figure 1 ^{18}F-FES uptake in MCF-7 and ZR-75-1 breast tumor-bearing mice. (A) Arrows show tumors. (B) Comparison of %ID/g between ZR-75-1 and MCF-7 breast tumor-bearing mice.

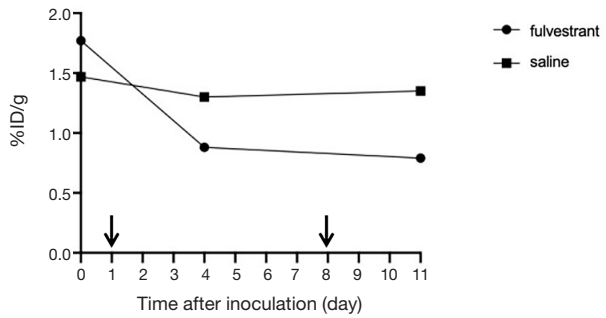

Figure 2 The time course of tumor uptake of ^{18}F-FES with or without fulvestrant treatment in ZR-75-1 breast tumor-bearing mice. (↓ : fulvestrant and saline injection time; square: experiment group; circle: control group).

too small to be delineated *in vivo*).

Immunohistochemistry

Using the Allred scoring system, the scores of ZR-75-1 breast tumor were 4.5±0.22. Thus, the positive expression of ER in ZR-75-1 tumors was confirmed by and consistent with PET-CT imaging (*Figure 4*).

Safety

Abnormal toxicity test

No abnormal reaction or death occurred in tumor-bearing mice at 48 hours after ^{18}F-FES administration. This result met the requirements of the abnormal toxicity test.

Radiation dose in human body

The main radioactive retention time data of each source organ in tumor-bearing mice are shown in *Table 1*. The retention time of ^{18}F-FES in the liver, small intestine and bladder were 0.0743, 0.1310 and 0.0847 MBq.h/MBq, respectively. In the heart, brain, kidney and spleen, the retention time was 0.0039, 0.0068, 0.0087 and 0.0021 MBq.h/MBq. OLINDA/EXM 2.0 software was used for computing the average absorbed dose of each organ in the adult female body. The average absorbed dose was relatively high in the gallbladder (0.616 mGy/MBq), small intestine (0.568 mGy/MBq) and bladder (0.0521 mGy/MBq). The values of the liver, uterus and ovaries were 0.0191, 0.0232 and 0.0204 mGy/MBq. Effective dose all over was calculated on the basis of the radiation weighting factor and tissue weighting factor provided by the ICRP 103 files, and the value was 0.016 mSv/MBq.

There was no statistical difference between the absorbed dose of each organ in this research and that measured directly in a healthy human body (t=1.138, P=0.27) (17).

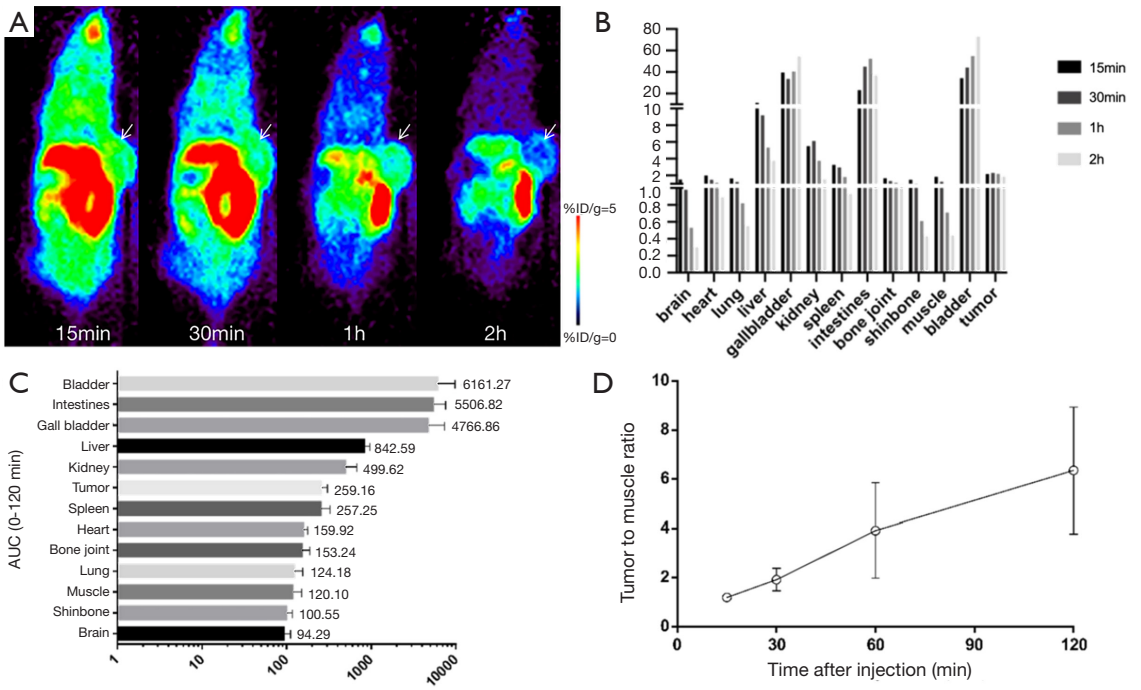

Figure 3 Biological distribution of ^{18}F-FES in tumor-bearing mice measured under isoflurane anesthesia (200 μCi per mouse). (A) ^{18}F-FES PET-CT coronal imaging of breast-cancer-bearing mice. Arrows indicate the tumor. (B) Biodistribution of ^{18}F-FES in breast-cancer-bearing mice at 15, 30, 60 and 120 minutes after injection. (C) 0–120 min AUC charted for each organ. (D) Target-to-muscle ratio.

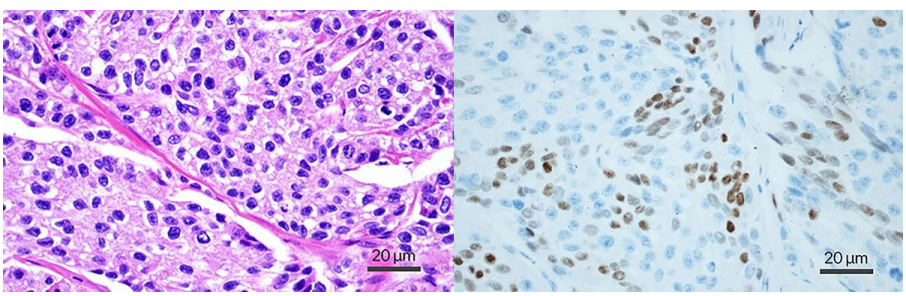

Figure 4 Hematoxylin-eosin staining and Immunohistochemistry staining of ZR-75-1 tumor cells.

Discussion

^{18}F-FES is a sensitive tracer to monitor ER expression of breast cancers (18). To provide a basis for clinical application, the biological properties of ^{18}F-FES were evaluated with ZR-75-1 breast tumor-bearing mice in this animal experiment. MCF-7 tumors have been widely used in current research, while ^{18}F-FES demonstrated significant uptake in ZR-75-1 tumors which were similar with MCF-7 tumors in this study and literature (1.87±0.13%ID/g) (19). Compared to MCF-7 cells, the receptors of ZR-75-1 cells are more similar to that of human, which ER and PR are all positive. Besides, ZR-75-1 breast tumor-bearing mice model, a appropriate ER-positive tumor model, has been used in FES imaging in a small range (20).

Fulvestrant, a new type of selective ER down-regulator (21), can compete with FES to bind ER. It reduces ER expression through the ubiquitin-proteasome pathway or direct block of the ER (22). Our experimental data showed that ^{18}F-FES uptake of the experimental group decreased significantly after fulvestrant administration, while there

Table 1 Radioactive retention time of each source organ in ZR-75-1 tumor-bearing mice

Source Organ	Kinetics Value [MBq.h/MBq]
Brain	6.76E-03
Gallbladder contents	1.78E-02
Small intestine	1.31E-01
Heart contents	3.87E-03
Kidneys	8.74E-03
Liver	7.43E-02
Lungs	7.59E-03
Cortical bone	1.90E-02
Trabecular bone	8.79E-03
Spleen	2.10E-03
Urinary bladder contents	8.47E-02
Reminder body	2.26E+00

was no significant change in tumor size on the third day after fulvestrant injection compared with baseline (Day 4 *vs.* Day 0, t=0.35, P=0.75). ^{18}F-FES-PET/CT may be more sensitive at predicting efficacy of endocrine therapy than tumor shrinkage (23). As has been stated, ^{18}F-FES could be a specific and sensitive imaging tracer of ER-positive tumors.

In the metabolic process of ^{18}F-FES in ZR-75-1 tumor-bearing mice, the highest uptake of ^{18}F-FES was in ER-positive tumors, except for excretory organs. This uptake characteristic was consistent with the research by previous researches (1.87±1.03 or 3.12±0.31 %ID/g in ER-positive tumors respectively) (19,24). FES is an analog of estradiol, and its metabolism is consistent with that of estradiol, which can selectively bind to ER receptors and transporters. High ^{18}F-FES uptake was observed in the liver and kidneys soon after the injection, which was consistent with previous reports (25). This is because ^{18}F-FES is mainly metabolized in the liver and rapidly cleared from the blood by the kidneys as early as 5 to 10 minutes after injection (26). At 15 minutes after injection, radioactivity levels in the blood declined slowly and remained fairly constant. ^{18}F-FES uptake in ER-negative organs, such as the lungs, muscle and brain, peaked at 15 minutes post injection, were lower than that in tumors. In addition, ^{18}F-FES uptake in bone was low which indicates minimal defluorination for ^{18}F-FES *in vivo* (27). The T/M ratio were increased over time, imaging 30 minutes after injection may produce good visualization of ER-positive tumors (28).

The distribution trend of FES was similar *in vivo* and *ex vivo*. However, ^{18}F-FES uptake of tumors measured *ex vivo* was lower than that *in vivo*. This may be due to the difference of sample volume, blood volume and tissue heterogeneity *in vivo* and *ex vivo* (23). Venema *et al.* (29) found a linear correlation of 0.78 between ^{18}F-FES uptake and IHC index, which was lower than that reported by Salem K (r^2=0.99) (30). These differences may be due to the heterogeneity of ER distribution leading to biopsy heterogeneity. Therefore, IHC cannot comprehensively characterize the ER expression of tumors, although ^{18}F-FES uptake of ER-positive tumors was consistent with semi-quantitative IHC in our study. ^{18}F-FES-PET/CT can reliably and noninvasively evaluate ER expression.

General and radiological safety was evaluated in this study. In line with the results of abnormal toxicity test, ^{18}F-FES had no adverse reactions and met the safety requirements. The average absorbed dose of each organ computed in the dosimetry study was generally lower than that measured in the human body (31). This may be due to discrepancy of FES metabolism between mice and humans. However, there was no statistical difference between derived dose and actual measurement in humans. Therefore, the absorbed doses in adult female body phantom can be extrapolated from mouse data. In clinical reports, the highest recommended dose of ^{18}F-FES is 2.22×10^8 Bq (32). According to our study, the effective dose of ^{18}F-FES was 0.016 mSv/MBq. Therefore, the systemic effective dose of ^{18}F-FES will be less than 5 mSv.

Limitations

There were several limitations in our present study. First, the quantitative analysis of ^{18}F-FES and IHC was not performed but the Allred scoring system was used as a semi-quantitative method. Second, the tumor-bearing mice utilized were limited, multiple tumor-bearing mice should be required for studying^{18}F-FES comprehensively in the future.

Conclusions

In summary, ^{18}F-FES is a safe and specific tracer for evaluating ER expression *in vivo*. The distribution of ^{18}F-FES is well correlated with traditional measurements *ex vivo*. It may be a predictor of endocrine therapy efficacy and

could be widely used in individualized treatment of breast cancer.

Acknowledgments

Funding: This work was supported by Jiangsu Key Medical Talents Fund (No. ZDRCB2016003), Jiangsu Provincial Health and Family Planning Commission Foundation No. Z201502 to TL, H2018029 to JS and Key Laboratory of Nuclear Medicine Ministry of Health, Jiangsu Key Laboratory of Molecular Nuclear Medicine (No. KF201501).

Footnote

Reporting Checklist: The authors have completed the ARRIVE reporting checklist. Available at http://dx.doi.org/10.21037/tcr-20-3228

Data Sharing Statement: Available at http://dx.doi.org/10.21037/tcr-20-3228

Peer Review File: Available at http://dx.doi.org/10.21037/tcr-20-3228

Conflicts of Interest: All authors have completed the ICMJE uniform disclosure form (available at http://dx.doi.org/10.21037/tcr-20-3228). The authors have no conflicts of interest to declare.

Ethical Statement: The authors are accountable for all aspects of the work in ensuring that questions related to the accuracy or integrity of any part of the work are appropriately investigated and resolved. All animal experiments were approved by the Institutional Animal Care and Use Committee of MITRO Biotech (AP-MIJ190019), in compliance with all national or institutional guidelines for the care and use of animals.

References

1. Bray F, Ferlay J, Soerjomataram I, et al. Global cancer statistics 2018: GLOBOCAN estimates of incidence and mortality worldwide for 36 cancers in 185 countries. CA Cancer J Clin 2018;68:394-424.
2. Siegel RL, Miller KD, Jemal A. Cancer statistics, 2020. CA Cancer J Clin 2020;70:7-30.
3. Fowler AM, Clark AS, Katzenellenbogen JA, et al. Imaging Diagnostic and Therapeutic Targets: Steroid Receptors in Breast Cancer. J Nucl Med 2016;57:75S-80S.
4. Xu D, Zhuang R, You L, et al. (18)F-labeled estradiol derivative for targeting estrogen receptor-expressing breast cancer. Nucl Med Biol 2018;59:48-55.
5. Sohail SK, Sarfraz R, Imran M, et al. Estrogen and Progesterone Receptor Expression in Breast Carcinoma and Its Association With Clinicopathological Variables Among the Pakistani Population. Cureus 2020;12:e9751.
6. Yang Z, Sun Y, Xu X, et al. The Assessment of Estrogen Receptor Status and Its Intratumoral Heterogeneity in Patients With Breast Cancer by Using 18F-Fluoroestradiol PET/CT. Clin Nucl Med 2017;42:421-7.
7. Sharangpani GM, Joshi AS, Porter K, et al. Semi-automated imaging system to quantitate estrogen and progesterone receptor immunoreactivity in human breast cancer. J Microsc 2007;226:244-55.
8. Lu Y, Tong Y, Huang J, et al. Primary 21-Gene Recurrence Score and Disease Outcome in Loco-Regional and Distant Recurrent Breast Cancer Patients. Front Oncol 2020;10:1315.
9. Hammond ME, Hayes DF, Dowsett M, et al. American Society of Clinical Oncology/College Of American Pathologists guideline recommendations for immunohistochemical testing of estrogen and progesterone receptors in breast cancer. J Clin Oncol 2010;28:2784-95.
10. Zhang Z, Tang P. Genomic Pathology and Biomarkers in Breast Cancer. Crit Rev Oncog 2017;22:411-26.
11. Jones EF, Hathi DK, Freimanis R, et al. Current Landscape of Breast Cancer Imaging and Potential Quantitative Imaging Markers of Response in ER-Positive Breast Cancers Treated with Neoadjuvant Therapy. Cancers (Basel) 2020;12:1511.
12. Chang HT, Chou CT, Lin YS, et al. Esculetin, a natural coumarin compound, evokes Ca(2+) movement and activation of Ca(2+)-associated mitochondrial apoptotic pathways that involved cell cycle arrest in ZR-75-1 human breast cancer cells. Tumour Biol 2016;37:4665-78.
13. Abdalla Elhassan SI. The five-year survival rate of breast

cancer at Radiation and Isotopes Centre Khartoum, Sudan. Heliyon 2020;6:e04615.
14. Qureshi A, Pervez S. Allred scoring for ER reporting and it's impact in clearly distinguishing ER negative from ER positive breast cancers. J Pak Med Assoc 2010;60:350-3.
15. Constantinescu CC, Sevrioukov E, Garcia A, et al. Evaluation of [18F]Mefway biodistribution and dosimetry based on whole-body PET imaging of mice. Mol Imaging Biol 2013;15:222-9.
16. Stabin MG, Sparks RB, Crowe E. OLINDA/EXM: the second-generation personal computer software for internal dose assessment in nuclear medicine. J Nucl Med 2005;46:1023-7.
17. Stabin MG, Siegel JA. RADAR Dose Estimate Report: A Compendium of Radiopharmaceutical Dose Estimates Based on OLINDA/EXM Version 2.0. J Nucl Med 2018;59:154-60.
18. van Kruchten M, de Vries E, Brown M, et al. PET imaging of oestrogen receptors in patients with breast cancer. Lancet Oncol 2013;14:e465-75.
19. Downer JB, Jones LA, Katzenellenbogen JA, et al. Effect of administration route on FES uptake into MCF-7 tumors. Nucl Med Biol 2001;28:397-9.
20. He S, Wang M, Yang Z, et al. Comparison of 18F-FES, 18F-FDG, and 18F-FMISO PET Imaging Probes for Early Prediction and Monitoring of Response to Endocrine Therapy in a Mouse Xenograft Model of ER-Positive Breast Cancer. Plos One 2016;11:e0159916.
21. O'Leary B, Cutts RJ, Huang X, et al. Circulating Tumor DNA Markers for Early Progression on Fulvestrant With or Without Palbociclib in ER+ Advanced Breast Cancer. J Natl Cancer Inst 2020;djaa087.
22. Bloomfield M, Louie MC. Chronic cadmium exposure decreases the dependency of MCF7 breast cancer cells on ERalpha. Sci Rep 2019;9:12135.
23. Lodge MA, Holt DP, Kinahan PE, et al. Performance assessment of a NaI(Tl) gamma counter for PET applications with methods for improved quantitative accuracy and greater standardization. Ejnmmi Phys 2015;2:11.
24. Bénard F, Ahmed N, Beauregard JM, et al. [18F] Fluorinated estradiol derivatives for oestrogen receptor imaging: impact of substituents, formulation and specific activity on the biodistribution in breast tumour-bearing mice. Eur J Nucl Med Mol Imaging 2008;35:1473-9.
25. Aliaga A, Rousseau JA, Ouellette R, et al. Breast cancer models to study the expression of estrogen receptors with small animal PET imaging. Nucl Med Biol 2004;31:761-70.
26. Paquette M, Lavallee E, Phoenix S, et al. Improved Estrogen Receptor Assessment by PET Using the Novel Radiotracer (18)F-4FMFES in Estrogen Receptor-Positive Breast Cancer Patients: An Ongoing Phase II Clinical Trial. J Nucl Med 2018;59:197-203.
27. Katzenellenbogen JA. PET Imaging Agents (FES, FFNP, and FDHT) for Estrogen, Androgen, and Progesterone Receptors to Improve Management of Breast and Prostate Cancers by Functional Imaging. Cancers (Basel) 2020;12:2020.
28. Talbot JN, Gligorov J, Nataf V, et al. Current applications of PET imaging of sex hormone receptors with a fluorinated analogue of estradiol or of testosterone. Q J Nucl Med Mol Imaging 2015;59:4-17.
29. Venema CM, Mammatas LH, Schroder CP, et al. Androgen and Estrogen Receptor Imaging in Metastatic Breast Cancer Patients as a Surrogate for Tissue Biopsies. J Nucl Med 2017;58:1906-12.
30. Salem K, Kumar M, Kloepping KC, et al. Determination of binding affinity of molecular imaging agents for steroid hormone receptors in breast cancer. Am J Nucl Med Mol Imaging 2018;8:119-26.
31. Mankoff DA, Peterson LM, Tewson TJ, et al. [18F] fluoroestradiol radiation dosimetry in human PET studies. J Nucl Med 2001;42:679-84.
32. Liao GJ, Clark AS, Schubert EK, et al. 18F-Fluoroestradiol PET: Current Status and Potential Future Clinical Applications. J Nucl Med 2016;57:1269-75.

Cite this article as: Ding Z, Xu X, Li T, Wang J, Sun J, Tang L. ZR-75-1 breast cancer models to study the utility of ^{18}F-FES by PET imaging. Transl Cancer Res 2021;10(3):1430-1438. doi: 10.21037/tcr-20-3228

